



HAL
open science

Sensor placement optimal for the precision of modal parameter estimation with subspace methods

Szymon Gres, Michael Döhler, Vasilis K. Dertimanis, Eleni Chatzi

► To cite this version:

Szymon Gres, Michael Döhler, Vasilis K. Dertimanis, Eleni Chatzi. Sensor placement optimal for the precision of modal parameter estimation with subspace methods. EUROODYN 2023 - 12th International Conference on Structural Dynamics, Jul 2023, Delft, Netherlands. pp.1-10. hal-04249271

HAL Id: hal-04249271

<https://inria.hal.science/hal-04249271>

Submitted on 19 Oct 2023

HAL is a multi-disciplinary open access archive for the deposit and dissemination of scientific research documents, whether they are published or not. The documents may come from teaching and research institutions in France or abroad, or from public or private research centers.

L'archive ouverte pluridisciplinaire **HAL**, est destinée au dépôt et à la diffusion de documents scientifiques de niveau recherche, publiés ou non, émanant des établissements d'enseignement et de recherche français ou étrangers, des laboratoires publics ou privés.



Distributed under a Creative Commons Attribution 4.0 International License

Sensor placement optimal for the precision of modal parameter estimation with subspace methods

Szymon Gres¹, Michael Döhler², Vasilis Dertimanis¹, and Eleni Chatzi¹

¹Department of Civil, Environmental and Geomatic Engineering, ETH Zürich, 8093 Zürich, Switzerland

²Univ. Gustave Eiffel, Inria, COSYS/SII, I4S, Campus de Beaulieu, 35042 Rennes, France

E-mail: szymon.gres@ibk.baug.ethz.ch

Abstract. In this paper we focus on sensor placement for output-only modal analysis, where the objective is to choose those sensor locations yielding a minimal variance in the identification of modal parameters from measurement data. It is heuristically shown that the variance of modal parameters estimated with data-driven subspace identification can be approximated solely based on the process and the measurement noise properties with the Kalman filter and the underlying system model, and is independent of data which are not available at the experimental design stage. The performance of the proposed approach is illustrated on an extensive Monte Carlo simulation for an illustrative example of a mechanical chain system.

1. Introduction

The design of an optimal sensor layout forms a classical problem in structural health monitoring, usually posed in the context of achieving a specific objective; for example, maximizing identifiability of a particular set of modes [1], maximizing detectability and localizability of a specific damage type [2, 3], increasing the precision of virtual sensing [4, 5], reducing the uncertainty in the modal parameter estimates [6, 7, 8], among many others. A common approach to attain those goals is to define performance criteria characterizing the objective; these typically relate to information theory-related metrics, such as entropy and mutual information, Fisher information on modal contributions, kinetic mode energy, Fisher information on specific monitoring parameters, and other criteria reflecting redundancy in the estimated parameters, e.g., mode shape correlations, among many more.

The precision in the estimation of modal parameters is afflicted by the typically unknown (non-measurable) ambient excitation and sensor noise. Some sensor placement strategies consider the statistical uncertainty of the modal parameters; however, only few approaches employ the actual noise properties of the system, and instead assume a certain distribution of the modal parameters in a Bayesian context [6, 7]. The objective of this paper is to develop a sensor placement strategy for modal parameter identification inferred via subspace methods that consider the actual noise properties of the system, such that the collected data can ensure maximum precision on the modal parameters, namely the natural frequencies and damping ratios. The proposed procedure is purely model-based, as no data are available at the experimental design-stage, and assumes the knowledge of the structural model and the noise

properties of the system, i.e., the covariance of the ambient excitation and the sensor noise. From this information, the expected modal parameter variance is inferred for any sensor layout, based on the model and the known noise properties, without the necessity of (simulating) data. The computed variance is then used as performance criterion to optimize the sensor layout.

The paper is organized as follows. Section 2 introduces the required models and background for subspace identification and uncertainty propagation. In Section 3, the modal parameter variance is derived based on the structural and noise models, and used as a performance criterion to select the optimal sensor placement. An application on a numerical simulation is presented in Section 4 to validate the developed uncertainty-based performance criterion for optimal sensor placement.

2. Modelling

In this section the system model, the modal parameter estimator and the underlying properties of the Kalman filter are recalled. Assume that the dynamic behavior of a linear time-invariant mechanical system excited with a white noise excitation can be represented by a discrete-time state-space model of order n

$$x_{k+1} = Ax_k + w_k \quad (1)$$

$$y_k = Cx_k + v_k, \quad (2)$$

where $x_k \in \mathbb{R}^n$ are the states, $y_k \in \mathbb{R}^r$ are the outputs, and $A \in \mathbb{R}^{n \times n}$, $C \in \mathbb{R}^{r \times n}$ are the state transition and observation matrices, respectively. The process noise $w_k \in \mathbb{R}^n$ and the measurement noise $v_k \in \mathbb{R}^r$ are modelled as zero-mean, Gaussian and white processes, of covariance and cross-covariance matrices

$$\begin{bmatrix} Q & S \\ S^T & R \end{bmatrix} = \mathbf{E} \left(\begin{bmatrix} w_k \\ v_k \end{bmatrix} \begin{bmatrix} w_k^T & v_k^T \end{bmatrix} \right). \quad (3)$$

Both noise processes are assumed to have finite fourth moments and to be persistently exciting [9]. The system is assumed to be stable, observable, and with distinct eigenvalues of A . Some of the aforementioned assumptions are discussed in detail in [10].

The i -th natural frequency f , damping ratio ζ and the observed mode shape φ of the underlying structural system are related to the i -th eigenvalue $\lambda = \exp(\lambda_c \tau)$ and the i -th eigenvector ϕ of A by

$$f = \frac{|\lambda_c|}{2\pi}, \quad \zeta = \frac{-\Re(\lambda_c)}{|\lambda_c|}, \quad \varphi = C\phi. \quad (4)$$

2.1. Kalman predictor model

Define the innovation $e_k = y_k - C\hat{x}_k \in \mathbb{R}^r$ and let K_k be the Kalman predictor gain to be specified later. A recursive filter to obtain one step-ahead state estimates \hat{x}_{k+1} writes

$$\hat{x}_{k+1} = A\hat{x}_k + K_k e_k, \quad (5)$$

$$y_k = C\hat{x}_k + e_k, \quad (6)$$

which is the state-space model in the innovation form. The Kalman predictor gain is derived to minimize the trace of the one step-ahead state prediction error covariance P_{k+1}

$$K_k = (AP_k C^T + S) (CP_k C^T + R)^{-1} \quad (7)$$

$$P_{k+1} = AP_k A^T + Q - K_k (AP_k C^T + S)^T, \quad (8)$$

where $P_k \stackrel{\text{def}}{=} \mathbf{E}((\hat{x}_k - x_k)(\hat{x}_k - x_k)^T)$, and $\Sigma_k^e \stackrel{\text{def}}{=} CP_{k|k-1}C^T + R$ is the innovation covariance. Furthermore, define the one step-ahead state prediction covariance $T_k \stackrel{\text{def}}{=} \mathbf{E}(\hat{x}_k \hat{x}_k^T)$, which satisfies the recursion [11]

$$T_{k+1} = AT_kA^T + (AT_kC^T - \Theta_k)(\Phi_k - CT_kC^T)^{-1}(AT_kC^T - \Theta_k)^T \quad (9)$$

with the state covariance $\Sigma_k^x = \mathbf{E}(x_k x_k^T)$, cross-covariance between states and outputs $\Theta_k = \mathbf{E}(x_{k+1} y_k^T)$ and output covariance $\Phi_k = \mathbf{E}(y_k y_k^T)$, satisfying the properties [12]

$$\Sigma_{k+1}^x = A\Sigma_k^x A^T + Q \quad (10)$$

$$\Theta_k = A\Sigma_k^x C^T + S \quad (11)$$

$$\Phi_k = C\Sigma_k^x C^T + R \quad (12)$$

and the relation between state covariance, state prediction error covariance and state prediction covariance [11]

$$T_k = \Sigma_k^x - P_k. \quad (13)$$

For $k \rightarrow \infty$, all matrices from Eq. (7)–(13) converge to their steady-state counterparts, where the index k is dropped. In particular, Σ^x can be obtained by solving the Lyapunov equation (10), and P and T can be obtained by solving the Ricatti equations (8) and (9), respectively. It should be noted that all these matrices can be computed based on knowledge of the model matrices (A, C, Q, R, S) and no actual data are required.

2.2. Estimated model

Definition 1 (Data matrix). Let $a_k \in \mathbb{R}^b$ be a discrete signal at time step k . The parameter p defines the ‘past’ and ‘future’ data horizons. For $0 \leq i \leq j \leq 2p - 1$ the data matrix $\mathcal{A}_{i|j}$ writes

$$\mathcal{A}_{i|j} = \frac{1}{\sqrt{N}} \begin{bmatrix} a_i & a_{i+1} & \dots & a_{i+N-1} \\ a_{i+1} & a_{i+2} & \dots & a_{i+N} \\ \vdots & \vdots & \vdots & \vdots \\ a_j & a_{j+1} & \dots & a_{j+N-1} \end{bmatrix} \in \mathbb{R}^{(j-i+1)b \times N}, \quad (14)$$

where N is the number of the considered data samples.

From $N + 2p$ samples of output data, define the data matrices $\mathcal{Y}^- = \mathcal{Y}_{0|p-1} \in \mathbb{R}^{pr \times N}$, $\mathcal{Y}^+ = \mathcal{Y}_{p|2p-1} \in \mathbb{R}^{pr \times N}$ and from the innovations define $\mathcal{E}^- = \mathcal{E}_{0|p-1} \in \mathbb{R}^{pr \times N}$, $\mathcal{E}^+ = \mathcal{E}_{p|2p-1} \in \mathbb{R}^{pr \times N}$. Furthermore, denote respectively the future and the past block-row matrices for the Kalman filter states as $\hat{\mathcal{X}}^- = \hat{\mathcal{X}}_{0|0}$, $\hat{\mathcal{X}}^+ = \hat{\mathcal{X}}_{p|p}$ and define the observability matrix $\Gamma \in \mathbb{R}^{pr \times n}$

$$\Gamma = \begin{bmatrix} C \\ CA \\ CA^2 \\ \vdots \\ CA^{p-1} \end{bmatrix}. \quad (15)$$

It holds

$$\mathcal{Y}^- = \Gamma \hat{\mathcal{X}}^- + \mathcal{K} \mathcal{E}^- + \mathcal{E}_{\mathcal{K}}^-, \quad \mathcal{Y}^+ = \Gamma \hat{\mathcal{X}}^+ + \mathcal{K} \mathcal{E}^+ + \mathcal{E}_{\mathcal{K}}^+, \quad (16)$$

where $\mathcal{K}\mathcal{E}^-$ and $\mathcal{K}\mathcal{E}^+$ are related to the innovation terms with $\mathcal{K} \in \mathbb{R}^{pr \times pr}$ being defined based on the steady state Kalman gain K , and $\mathcal{E}_{\mathcal{K}}^-$ and $\mathcal{E}_{\mathcal{K}}^+$ are the remainder terms that are related to the difference to the actual non-steady state Kalman gain K_k , with

$$\mathcal{K} = \begin{bmatrix} \mathcal{I}_r & 0 & \dots & 0 \\ CK & \mathcal{I}_r & \dots & 0 \\ \dots & \dots & \dots & \dots \\ CA^{p-2}K & CA^{p-3}K & \dots & \mathcal{I}_r \end{bmatrix}, \quad \mathcal{K}_l = \begin{bmatrix} \mathcal{I}_r & 0 & \dots & 0 \\ CK_l & \mathcal{I}_r & \dots & 0 \\ \dots & \dots & \dots & \dots \\ CA^{p-2}K_l & CA^{p-2}K_{l+1} & \dots & \mathcal{I}_r \end{bmatrix},$$

where the l -th columns of $\mathcal{E}_{\mathcal{K}}^-$ and $\mathcal{E}_{\mathcal{K}}^+$ respectively are [13]

$$[\mathcal{E}_{\mathcal{K}}^-]_l = (\mathcal{K}_{l-1} - \mathcal{K})[\mathcal{E}^-]_l, \quad [\mathcal{E}_{\mathcal{K}}^+]_l = (\mathcal{K}_{l-1+p} - \mathcal{K})[\mathcal{E}^+]_l. \quad (17)$$

Columns $[\mathcal{E}_{\mathcal{K}}^-]_l$ and $[\mathcal{E}_{\mathcal{K}}^+]_l$ converge to zero as p grows, since the non-steady state Kalman gain K_l converges to the steady state gain K . The projection of the future data matrix \mathcal{Y}^+ onto the past matrix \mathcal{Y}^- yields the factorization

$$\mathcal{H} = \mathcal{Y}^+/\mathcal{Y}^- = \hat{\Gamma}\hat{\mathcal{X}}^+, \quad (18)$$

where the observability matrix estimate $\hat{\Gamma}$ and the Kalman filter state sequence $\hat{\mathcal{X}}^+$ can be retrieved from SVD

$$\mathcal{H} = [U_1 \ U_2] \begin{bmatrix} \Sigma_1 & 0 \\ 0 & \Sigma_2 \end{bmatrix} \begin{bmatrix} V_1^T \\ V_2^T \end{bmatrix}, \quad \hat{\Gamma} = U_1 \Sigma_1^{1/2}, \quad \hat{\mathcal{X}}^+ = \Sigma_1^{1/2} V_1^T. \quad (19)$$

The state transition matrix can be obtained from the regression

$$\hat{A} = \hat{\mathcal{X}}_s^+ \hat{\mathcal{X}}^{+\dagger}, \quad (20)$$

where $\hat{\mathcal{X}}_s^+ = \hat{\Gamma}^\dagger \mathcal{H}$, $\hat{\Gamma}^\dagger$ denotes the observability matrix without the last block row, and $\mathcal{H} = \underline{\mathcal{Y}}^+/\underline{\mathcal{Y}}^-$ with $\underline{\mathcal{Y}}^+ = \mathcal{Y}_{p+1|2p-1}$ and $\underline{\mathcal{Y}}^- = \mathcal{Y}_{0|p}$ [12].

2.3. Uncertainty propagation

The uncertainty related to the estimation of A and the underlying estimates of the modal parameters can be quantified with the statistical delta method, by propagating the sample covariance of data covariance onto the chosen estimates [14]. Let a data covariance matrix be defined as $\mathcal{H}^s = \mathcal{H}\mathcal{H}^T$. Entries of this covariance matrix are asymptotically Gaussian

$$\sqrt{N} \text{vec}(\hat{\mathcal{H}}^s - \mathcal{H}^s) \rightarrow \mathcal{N}(0, \Sigma_{\mathcal{H}^s}), \quad (21)$$

where $\Sigma_{\mathcal{H}^s}$ is the asymptotic covariance of $\text{vec}(\hat{\mathcal{H}}^s)$, and $\text{vec}(\cdot)$ denotes the column stacking vectorization operator. An estimate $\hat{\Sigma}_{\mathcal{H}^s}$ of the covariance can be easily evaluated by the sample covariance based on partitions of the available data. The propagation of $\hat{\Sigma}_{\mathcal{H}^s}$ onto the modal parameter estimates is then based on the first-order perturbation theory, using the fact that estimates $(\hat{f}, \hat{\zeta})$ are a function of the data covariance matrix $\hat{\mathcal{H}}^s$. It then follows

$$\sqrt{N} \text{vec}(\hat{f} - f) \rightarrow \mathcal{N}(0, \mathcal{J}_{\mathcal{H}^s}^f \Sigma_{\mathcal{H}^s} \mathcal{J}_{\mathcal{H}^s}^{fT}), \quad \sqrt{N} \text{vec}(\hat{\zeta} - \zeta) \rightarrow \mathcal{N}(0, \mathcal{J}_{\mathcal{H}^s}^\zeta \Sigma_{\mathcal{H}^s} \mathcal{J}_{\mathcal{H}^s}^{\zeta T}), \quad (22)$$

where $\mathcal{J}_{\mathcal{H}^s}^f$, $\mathcal{J}_{\mathcal{H}^s}^\zeta$ are the derivatives of the natural frequency and damping ratio with respect to \mathcal{H}^s obtained by perturbing the functional relationship between \mathcal{H}^s and (f, ζ) analytically, and neglecting the higher-order terms, even when the functional relationship is not explicit. Subsequently, covariance expressions for the estimates satisfy

$$\hat{\sigma}_f \approx \hat{\mathcal{J}}_{f, \mathcal{H}^s} \hat{\Sigma}_{\mathcal{H}^s} \hat{\mathcal{J}}_{f, \mathcal{H}^s}^T, \quad \hat{\sigma}_\zeta \approx \hat{\mathcal{J}}_{\zeta, \mathcal{H}^s} \hat{\Sigma}_{\mathcal{H}^s} \hat{\mathcal{J}}_{\zeta, \mathcal{H}^s}^T. \quad (23)$$

With this principle, the uncertainties of the output covariances can be propagated step by step through the subspace identification algorithm down to the modal parameters. The analytical sensitivities are derived in detail in [15], with a computationally efficient algorithm proposed in [16].

2.4. Problem statement

The objective is to find a sensor layout – based on a model at the design stage of an experiment – that yields a minimal variance of the modal parameters when they will be identified from the actual data at the selected sensor positions with subspace-based system identification. The proposed procedure is purely model-based, as no data are available at the experimental design-stage, and assumes the knowledge of the system matrix A , the type and number of sensors used (acceleration, velocity or displacement sensors), as well as the knowledge of the noise properties of the system, i.e., matrices (Q, R, S) . From this information, the expected modal parameter variance is inferred for a given sensor layout encoded in C , based on the model and the known noise properties of the system. An objective function is then designed, and minimized, to attain a minimal variance of modal parameters to be-identified from data. The objective function is designed based on a performance criterion using the accumulated coefficients of variation of the frequencies and damping ratios

$$F(C) = \text{COV}_f + \text{COV}_\zeta, \quad (24)$$

where $\text{COV}_f = \sum_{i=1}^n \frac{\sigma_{f_i}}{f_i}$ and $\text{COV}_\zeta = \sum_{i=1}^n \frac{\sigma_{\zeta_i}}{\zeta_i}$ are implicitly a function of C , which contains the sensor positions in-question, and n is the number of modes. The optimal sensor layout is then obtained as

$$C^{\text{opt}} = \arg \min_C F(C). \quad (25)$$

3. Variance approximation

The estimation of matrix A with the subspace identification method is described in Section 2.2. For an analytical evaluation of the variance of \hat{A} , solely based on the model matrices (A, C, Q, R, S) , a slightly different estimation problem is considered; which, however, is close to the one of subspace identification. For this we use the regression on the Kalman filter states to estimate A , in order to link the noise properties (Q, R, S) via the Kalman filter to the estimation covariance of \hat{A} .

Define \hat{X}^+ and \hat{X}^- by removing the first and the last sample from \hat{X}^- (see Section 2.2), respectively, then

$$\hat{X}^+ = A\hat{X}^- + KE^- \quad (26)$$

with

$$\hat{X}^+ = \frac{1}{\sqrt{N}} [\hat{x}_2 \quad \dots \quad \hat{x}_N], \quad \hat{X}^- = \frac{1}{\sqrt{N}} [\hat{x}_1 \quad \dots \quad \hat{x}_{N-1}], \quad \hat{E}^- = \frac{1}{\sqrt{N}} [e_1 \quad \dots \quad e_{N-1}].$$

From this relationship, an estimate of A can be obtained by the regression

$$\hat{A} = \hat{X}^+ \hat{X}^{-\dagger} = \hat{X}^+ \hat{X}^{-T} (\hat{X}^- \hat{X}^{-T})^{-1}. \quad (27)$$

To analyze its covariance, we start by analyzing the rows of \hat{A} . For ease of the notation, the transpose of Eq. (27) is taken, and the columns \hat{A}_i^T of $\hat{A}^T = [\hat{A}_1^T \quad \dots \quad \hat{A}_n^T]$ are considered. Accordingly, define the i -th state sequence \hat{X}_i^{+T} as the i -th column of \hat{X}^{+T} , and K_i^T as the i -th column of K^T . It follows

$$\hat{A}_i^T = (\hat{X}^- \hat{X}^{-T})^{-1} \hat{X}^- \hat{X}_i^{+T} \quad (28)$$

$$= (\hat{X}^- \hat{X}^{-T})^{-1} \hat{X}^- \underbrace{(\hat{X}_i^{+T} - \hat{X}^{-T} A_i^T)}_{\stackrel{\text{def}}{=} r_i} + A_i^T \quad (29)$$

where r_i is the residual of the regression. Let the covariance of \hat{A}_i^T be defined as $\Sigma_{A_i^T} = \mathbf{E} \left((\hat{A}_i^T - A_i^T)(\hat{A}_i - A_i) \right)$. Following Eq. (29), this covariance yields

$$\Sigma_{A_i^T} = \mathbf{E} \left((\hat{X}^- \hat{X}^{-T})^{-1} \hat{X}^- r_i r_i^T \hat{X}^{-T} (\hat{X}^- \hat{X}^{-T})^{-1} \right).$$

Assume now that $\hat{X}^- \hat{X}^{-T} \rightarrow T$ has converged, then

$$\Sigma_{A_i^T} = T^{-1} \mathbf{E} \left(\hat{X}^- r_i r_i^T \hat{X}^{-T} \right) T^{-1} \quad (30)$$

Based on Eq. (26), the residual writes

$$r_i = \hat{E}^{-T} K_i^T,$$

and the product $\hat{X}^- r_i$ in Eq. (30) yields

$$\begin{aligned} \hat{X}^- r_i &= \frac{1}{N} \sum_{j=1}^{N-1} \hat{x}_j e_j^T K_i^T, \\ \mathbf{E} \left(\hat{X}^- r_i r_i^T \hat{X}^{-T} \right) &= \frac{1}{N^2} \mathbf{E} \left(\left(\sum_{j=1}^{N-1} \hat{x}_j e_j^T K_i^T \right) \left(\sum_{l=1}^{N-1} \hat{x}_l e_l^T K_i^T \right)^T \right) \end{aligned}$$

Thanks to the presence of the innovation in this term, the expected value of the cross terms is zero for $j \neq l$, simplifying to

$$\mathbf{E} \left(\hat{X}^- r_i r_i^T \hat{X}^{-T} \right) = \frac{1}{N^2} \mathbf{E} \left(\sum_{j=1}^{N-1} \hat{x}_j e_j^T K_i^T K_i e_j \hat{x}_j^T \right).$$

Again thanks to the innovation, the terms in the sum are independent, leading to

$$\mathbf{E} \left(\hat{X}^- r_i r_i^T \hat{X}^{-T} \right) = \frac{1}{N^2} \sum_{j=1}^{N-1} \mathbf{E} \left(\hat{x}_j e_j^T K_i^T K_i e_j \hat{x}_j^T \right).$$

Since $e_j^T K_i^T$ is a scalar, the terms can be swapped, and since the innovation is independent from the state predictions, this yields

$$\begin{aligned} \mathbf{E} \left(\hat{X}^- r_i r_i^T \hat{X}^{-T} \right) &= \frac{1}{N^2} \sum_{j=1}^{N-1} \mathbf{E} \left(\hat{x}_j \hat{x}_j^T K_i e_j e_j^T K_i^T \right) \\ &= \frac{1}{N} T K_i \Sigma^e K_i^T \end{aligned}$$

in the steady state. Plugging this term back into Eq. (30), the covariance of \hat{A}_i^T can be approximated as

$$\Sigma_{A_i^T} = \frac{1}{N} T^{-1} K_i \Sigma^e K_i^T.$$

Analogously, the covariance between different columns of \hat{A}^T can be developed as

$$\Sigma_{A_i^T, A_l^T} = \frac{1}{N} T^{-1} K_i \Sigma^e K_l^T.$$

Based on these results, the covariance of $\text{vec}(\hat{A}^T)$ can be directly assembled, leading to

$$\Sigma_{A^T} = \frac{1}{N} (K \Sigma^e K^T) \otimes T^{-1}, \quad (31)$$

where $\text{vec}(\cdot)$ is the column stacking vectorization operator, and \otimes denotes the Kronecker product. It should be noted that this covariance is an approximation of the actual asymptotic covariance of an estimate of A from subspace identification, which is due to the approximation in (30) and the slightly different estimation of A in (20) when compared to estimating it from the observability matrix or from the full regression together with C [12]. Whereas the obtained approximation in (31) is a simple expression, the complete (and much more complex) analysis of the asymptotic variance is made e.g. in [17].

The asymptotic covariance Σ_{A^T} is then used to compute the variances of the natural frequencies and damping ratios, where the related sensitivities are obtained using the first-order perturbation theory. This allows to compute the coefficients of variation of the natural frequencies and damping ratios in Eq. (24) for any sensor placement. The optimal sensor placement is then chosen such that it minimizes Eq. (24). For the proof of concept, an exhaustive search over all possible sensor layouts is made in the following; however more efficient methods can be easily adopted in this context, like genetic algorithms [2], for examples see [18].

4. Application

In this section, the proposed sensor placement scheme is validated on an example of a 20 DOF mechanical chain-like system. The system is modeled with spring stiffness $k_i = 100$, mass $m_i = 1/20$ and a proportional damping matrix such that all modes have a damping ratio of 2%. The chain is excited by a white noise signal acting at all DOFs and the output accelerations are sampled with a frequency $f_s = 50$ Hz. A sketch of the system is depicted in Figure 1.

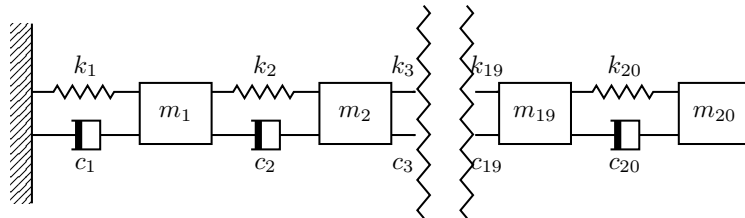


Figure 1. A sketch of a 20 DOF chain system.

The focus of this study is to find a sensor configuration that yields a minimal variance of the modal parameter estimates. For this purpose three sensors are considered. While an exhaustive search for the optimal placement is in general a computationally demanding task due to a large number of possible combinations, it is still feasible for selecting 3 sensors at 20 possible locations and considered hereafter for illustration purposes. The application comprises three parts; firstly, the uncertainty related to the state matrix obtained after Eq. (31) is propagated onto the natural frequencies and damping ratios, for every sensor configuration. Subsequently, two different sensor configurations are chosen and the related variance estimates are compared to the corresponding variances obtained from Monte Carlo sampling the natural frequencies and damping ratios obtained in a regression Eq. (27). Lastly, the estimated variances are compared with the variance obtained from Monte Carlo sampling of modal parameter estimated by means of data-driven subspace identification after Eq. (20).

The asymptotic variance of the natural frequencies and damping ratios is obtained as a function of the covariance of the state matrix (31), and the related sensitivities are obtained using the first-order perturbation theory. The left part of Figure 2 illustrates the sum of the Coefficients of Variation (COV) of the natural frequency and the damping ratio, COV_f and COV_ζ respectively, for each sensor configuration. It can be viewed that COV_f and COV_ζ change with the sensor configuration and that 8/1140 configurations exhibit relatively low variances. Those 8 configurations are then exploited for validation purposes in the remainder of this work. The right part of Figure 2 illustrates the COV_f and COV_ζ for two sensor configurations exhibiting low and high variances; the configurations 412 and 1140 respectively. It can be observed that while the difference between COV is small for the low-order modes, it is increased by a few orders of magnitude for the high-order modes.

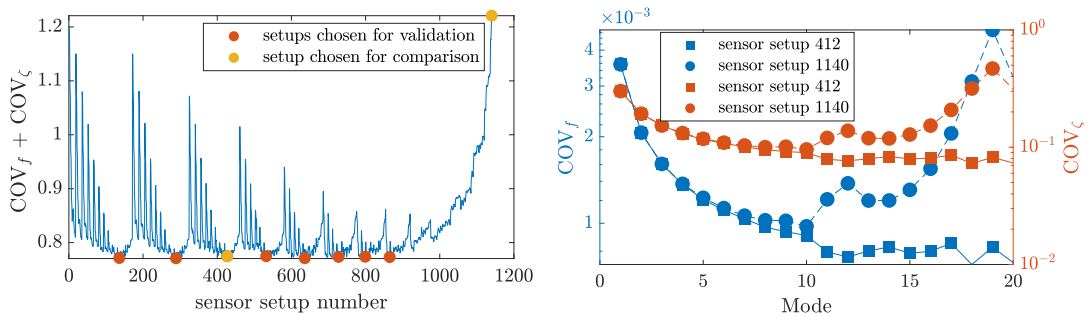


Figure 2. Sum of COV of the natural frequencies and damping ratios for every sensor setup (left). COV of the natural frequency for each mode for two chosen sensor configurations (right).

Figure 3 illustrates a comparison of Monte Carlo histograms for two sensor configurations. It can be seen that the variance of histograms is encompassed by the theoretical variance of the parameter obtained from the noise properties of the Kalman filter. In addition, differences between histograms are the largest for the higher-order modes, which agrees with the trend depicted in Figure 2.

Lastly, a comparison between the uncertainties obtained from sampling the subspace identification and the asymptotic uncertainties obtained using Eq. (31) is depicted in Figure 4. The left part of Figure 4 shows that while the magnitude of the COV is different, the general trend between two approaches is similar. The right part of Figure 4 illustrates a mean error on the variances obtained from sampling the subspace identification estimates and the proposed approach, for 8 sensor setups chosen for the validation. It can be viewed that for most of the validated setups the mean error oscillates between 10 – 15%, which can be related to the convergence of the Monte Carlo histograms.

5. Conclusions

In this paper a model-based sensor placement strategy was devised with the objective of minimizing the variance of modal parameters, which are to-be obtained from data. It was shown that the variance of modal parameters estimated with data-driven subspace identification can be approximated solely based on the process and the measurement noise properties using the Kalman filter and the underlying system model, and does not require actual data which are not available at the experimental design stage. The performance of the proposed approach was illustrated on an extensive Monte Carlo simulation conducted for the illustrative case of a mechanical chain system. Future work will comprise a formal comparison between the variance obtained with the proposed approach and the asymptotic results from [19], and an application to optimal sensor placement in a large-scale mechanical system.

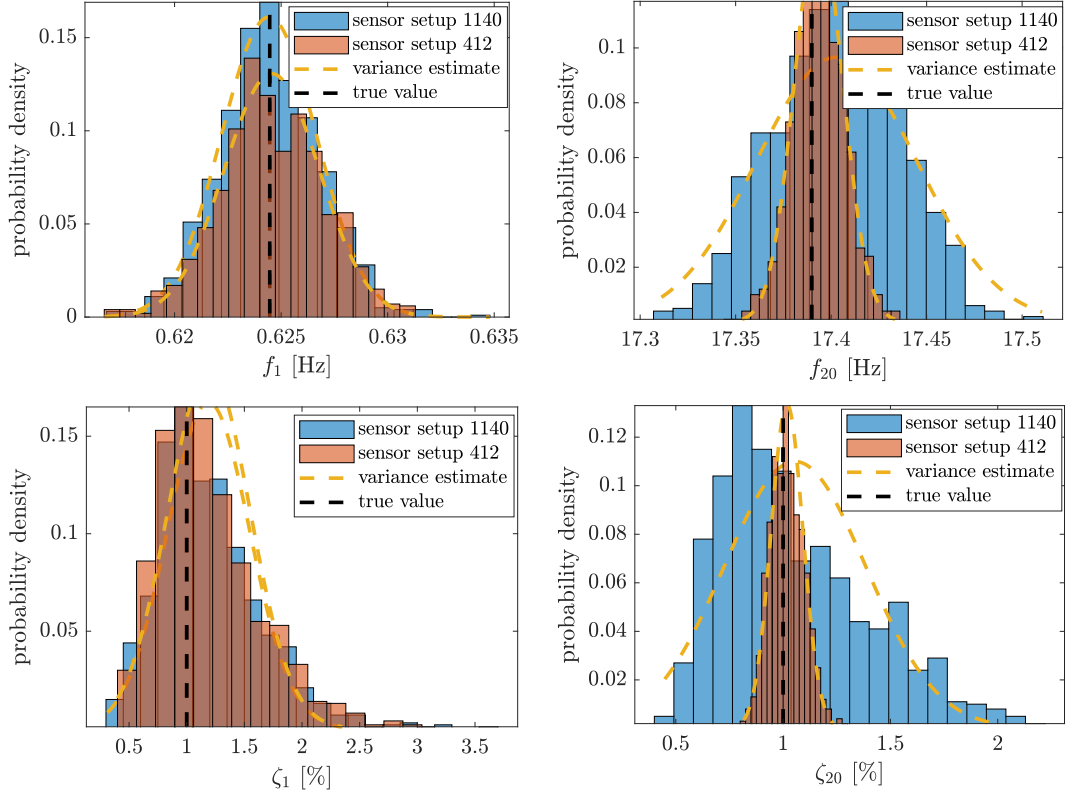


Figure 3. Monte Carlo histograms of the natural frequencies and damping ratios for two sensor configurations.

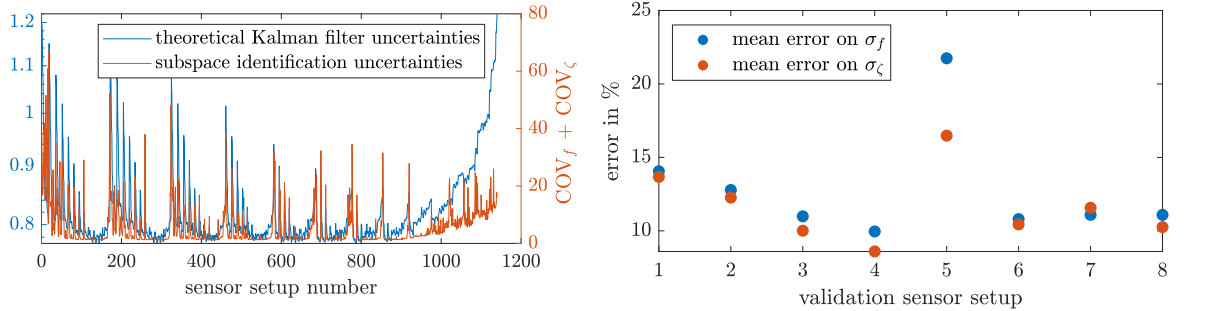


Figure 4. Sum of COV_f and COV_ζ obtained using the proposed approach and the data-driven subspace identification (left). Mean error between the σ_f and σ_ζ obtained using the proposed approach and the data-driven subspace identification (right).

References

- [1] D. C. Kammer, Sensor placement for on-orbit modal identification and correlation of large space structures, *Journal of Guidance, Control, and Dynamics* 14 (2) (1991) 251–259.
- [2] A. Mendler, M. Döhler, C. E. Ventura, Sensor placement with optimal damage detectability for statistical damage detection, *Mechanical Systems and Signal Processing* 170 (2022) 108767.
- [3] M. Ulriksen, D. Bernal, Sensor distributions for structural monitoring: a correlation study, in: N. Maia, M. Neves, R. Sampaio (Eds.), *Proceedings of the International Conference on Structural Engineering Dynamics - ICEDyn 2017*, ICEDyn, 2017.
- [4] V. Tzoumas, A. Jadbabaie, G. J. Pappas, Sensor placement for optimal kalman filtering: Fundamental limits, submodularity, and algorithms, in: *2016 American Control Conference (ACC)*, 2016, pp. 191–196.

doi:10.1109/ACC.2016.7524914.

- [5] T. Tamarozzi, E. Risaliti, W. Rottiers, W. Desmet, et al., Noise, ill-conditioning and sensor placement analysis for force estimation through virtual sensing, in: In International Conference on Noise and Vibration Engineering (ISMA2016),, 2016, pp. 1741–1756.
- [6] C. Papadimitriou, Optimal sensor placement methodology for parametric identification of structural systems, *Journal of Sound and Vibration* 278 (4) (2004) 923–947.
- [7] C. Papadimitriou, G. Lombaert, The effect of prediction error correlation on optimal sensor placement in structural dynamics, *Mechanical Systems and Signal Processing* 28 (2012) 105–127, interdisciplinary and Integration Aspects in Structural Health Monitoring.
- [8] M. Ulriksen, D. Bernal, L. Damkilde, in: A. Güemes (Ed.), *Proceedings of 8th European Workshop On Structural Health Monitoring (EWSHM 2016)*, Universidad Politécnica de Madrid, 2016.
- [9] R. Bitmead, Persistence of excitation conditions and the convergence of adaptive schemes, *IEEE Transactions on Information Theory* 30 (2) (1984) 183–191.
- [10] A. Benveniste, L. Mevel, Nonstationary consistency of subspace methods, *IEEE Transactions on Automatic Control* 52 (6) (2007) 974–984.
- [11] B. Anderson, J. B. Moore, *Optimal Filtering*, Prentice-Hall, Englewood Cliffs, N.J., 1979.
- [12] P. van Overschee, B. de Moor, *Subspace Identification for Linear Systems*, 1st Edition, Springer, 1996.
- [13] S. Greš, M. Döhler, P. Andersen, L. Mevel, Kalman filter-based subspace identification for operational modal analysis under unmeasured periodic excitation, *Mechanical Systems and Signal Processing* 146 (2021) 106996.
- [14] G. Casella, R. L. Berger, *Statistical Inference*, 2nd Edition, Cengage Learning, 2001.
- [15] E. Reynders, R. Pintelon, G. De Roeck, Uncertainty bounds on modal parameters obtained from stochastic subspace identification, *Mechanical Systems and Signal Processing* 22 (4) (2008) 948 – 969.
- [16] M. Döhler, L. Mevel, Efficient multi-order uncertainty computation for stochastic subspace identification, *Mechanical Systems and Signal Processing* 38 (2) (2013) 346–366.
- [17] D. Bauer, M. Deistler, W. Scherrer, Consistency and asymptotic normality of some subspace algorithms for systems without observed inputs, *Automatica* 35 (7) (1999) 1243 – 1254.
- [18] W. Ostachowicz, R. Soman, P. Malinowski, Optimization of sensor placement for structural health monitoring: a review, *Structural Health Monitoring* 18 (3) (2019) 963–988.
- [19] A. Chiuso, G. Picci, The asymptotic variance of subspace estimates, *Journal of Econometrics* 118 (1) (2004) 257 – 291.